Neuron, Vol. 36, 955–968, December 5, 2002, Copyright ©2002 by Cell Press

Probabilistic Decision Making by Slow Reverberation in Cortical Circuits

Xiao-Jing Wang[1]
Volen Center for Complex Systems
Brandeis University
Waltham, Massachusetts 02254

Summary

Recent physiological studies of alert primates have revealed cortical neural correlates of key steps in a perceptual decision-making process. To elucidate synaptic mechanisms of decision making, I investigated a biophysically realistic cortical network model for a visual discrimination experiment. In the model, slow recurrent excitation and feedback inhibition produce attractor dynamics that amplify the difference between conflicting inputs and generates a binary choice. The model is shown to account for salient characteristics of the observed decision-correlated neural activity, as well as the animal's psychometric function and reaction times. These results suggest that recurrent excitation mediated by NMDA receptors provides a candidate cellular mechanism for the slow time integration of sensory stimuli and the formation of categorical choices in a decision-making neocortical network.

Introduction

To generate cognitively based behavior, the brain relies on decision-making processes to interpret sensory stimuli, weigh evidence for choice alternatives, and form a perceptual decision or action selection. In order to unravel the neural mechanisms of decision making, neuroscientists have developed experimental approaches combining physiological and psychophysical techniques. While an alert monkey performs a task of perceptual discrimination or categorization or makes target selection for motor response, psychophysical data are collected to quantitatively measure the animal's performance. At the same time and under the same conditions, electrophysiological recordings are carried out to link the animal's behavior to single neural activity in specific brain areas (for reviews, see Parker and Newsome, 1998; Romo and Salinas, 2000; Schall, 2001).

In a visual motion discrimination task, the monkey is trained to make a judgment about the direction of motion in a near-threshold stochastic random dot display and to report the perceived direction with a saccadic eye movement. Physiological and microstimulation experiments have established that extrastriate visual cortex plays a critical role in visual motion processing. Evidence suggests that neurons in the area MT/MST encode the motion stimulus (Newsome et al., 1989; Salzman et al., 1990; Britten et al., 1992, 1993, 1996; Shadlen et al., 1996), and the decision process itself occurs downstream from MT/MST. A likely decision-making circuit is the posterior parietal cortex (area LIP), which receive inputs from MT/MST and which carries high-level signals for guiding saccadic eye movement (the motor output of the animal's decision). Indeed, Shadlen and Newsome found that activity of LIP cells signals the monkey's perceptual choice in both correct and error trials (Shadlen and Newsome, 1996, 2001). Activity of LIP neurons showed a slow ramping time course during stimulus viewing and persisted throughout a delay between the stimulus and the monkey's saccadic response. LIP neurons do not simply reflect sensory signals, because their activity is correlated with what the monkey decides, when the decision varies from trial to trial even at zero stimulus coherence. LIP neuronal activity cannot be purely a motor signal either, since its time course varies systematically with the motion signal strength (the quality of the sensory information), even though the saccadic motor output is basically the same (Shadlen and Newsome, 2001).

Similar decision-correlated neural activity has been reported in prefrontal cortex during the same visual motion discrimination task (Kim and Shadlen, 1999) and in medial premotor cortex during a vibrotactile discrimination task (Romo et al., 1997; Hernández et al., 2002). Assuming that the neural activity signaling decisions is generated within a cortical circuit, an intriguing question is: what are the basic cellular and synaptic mechanisms of a decision-making circuit? A clue comes from the observation that in the same (parietal, prefrontal, premotor) cortical areas, neurons generally show elevated persistent activity during a delay period of a few seconds, when the animal is required to actively hold the information of a sensory cue in working memory. Therefore, networks endowed with persistent activity may represent a class of cortical circuits capable of performing stimulus integration and categorical decision choice. I investigated this hypothesis by using a biophysically based recurrent cortical network model of spiking neurons for the visual motion discrimination experiment (Shadlen and Newsome, 1996, 2001; Roitman and Shadlen, 2002). As shown in this paper, slow synaptic reverberation mediated by NMDA receptors and winner-take-all competition mediated by feedback inhibition generate attractor dynamics that reproduces both neurophysiological and psychophysical data. This work suggests that slow attractor networks provide a theoretical framework for understanding time integration of inputs and formation of categorical choice in decision-making neocortical circuits.

Results

Simulation of the Delayed Visual Discrimination Experiment

A recurrent cortical network model (Amit and Brunel, 1997; Brunel and Wang, 2001) was used to simulate decision-correlated activity of LIP neurons in the delayed visual motion discrimination experiment (Shadlen and Newsome, 2001). The model displays mnemonic

[1]Correspondence: xjwang@brandeis.edu

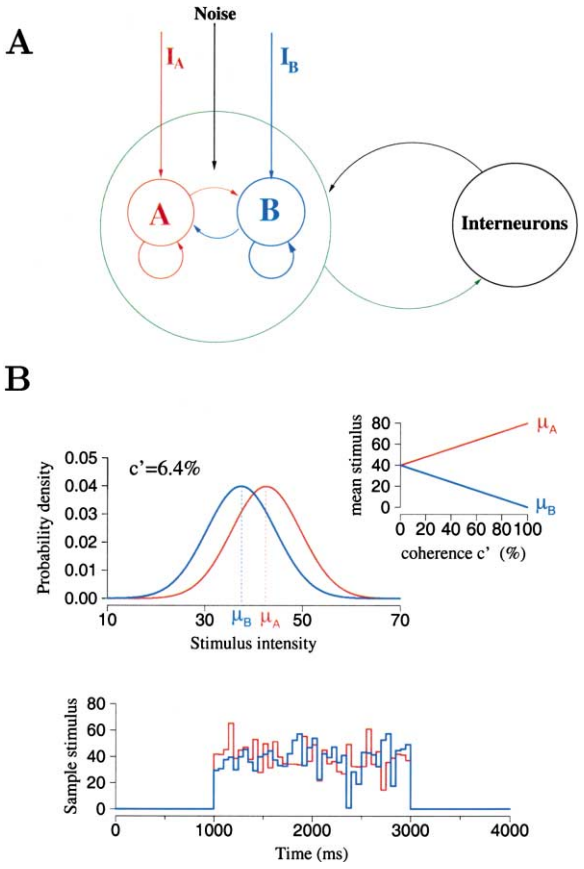

Figure 1. Model Architecture and Coherence-Dependent Stochastic Inputs

(A) Schematic depiction of the model. There are two pyramidal cell groups (A and B), each of which is selective to one of the two stimuli (mimicking motion to the right or left). Within each pyramidal neural group there is strong recurrrent excitatory connections that can sustain persistent activity triggered by a transient preferred stimulus. The two neural groups compete through feedback inhibition from interneurons.

(B) Top: the inputs are Poisson rates that vary in time and obey Gaussian distributions, with means μ_A and μ_B and with standard deviation σ. The means μ_A and μ_B depend on the coherence level linearly (insert). Bottom: an example of stochastic inputs to neural groups A and B with $\mu_0 = 40$ and $\sigma = 10$ in Hz, $c' = 6.4\%$. At every 50 ms, the two stimuli are independently resampled using their Gaussian distributions, so that the inputs vary stochastically in time. If $\sigma = 0$, the two inputs would be constant in time.

persistent activity, consistent with the fact that in working memory tasks LIP neurons show direction-selective sustained activity during a delay period (Shadlen and Newsome, 2001; Gnadt and Andersen, 1988; Colby et al., 1996; Chafee and Goldman-Rakic, 1998). For the sake of clarity, to simulate a two-choice decision task, I used a minimal version of the model that contains two neural groups: each is selective to one of the two motion directions (e.g., A, left motion; B, right motion). Strong recurrent excitatory connections within a neural group are capable of generating self-sustained persistent activity. There is also a competition between the two neural groups, due to the shared feedback inhibition from interneurons (Figure 1A). All neurons receive a large amount of background Poisson inputs and fire spontaneously at a few hertz.

During stimulation, both neural groups receive stochastic Poisson inputs at rates $s_A(t)$ and $s_B(t)$, respectively, mimicking the outputs from MT cells. The stimuli $s_A(t)$ and $s_B(t)$ (Figure 1B) vary in time; their distributions are Gaussian with a mean of μ_A and μ_B, respectively, and a standard deviation σ (equal to 4 unless specified otherwise). This presentation of MT outputs is clearly an oversimplication; it ignores such issues as pooling and noise correlation between MT cells (Zohary et al., 1994; Shadlen et al., 1996; Bair et al., 2001). However, the objective here is to study the decision-making behavior of the model, with the simplest form stimulus encoding by MT neurons. It is known that the response of an MT neuron increases with the input coherence c' for stimulus in its preferred direction and decreases with c' for stimulus in the direction 180° opposite (the "null" direction) (Britten et al., 1993, 1996). I implemented this dependence by assuming linear relations $\mu_A = \mu_0 + \rho_A c'$ and $\mu_B = \mu_0 - \rho_B c'$. For most of the simulations, I used $\rho_A = \rho_B = \mu_0/100$, in which case $c' = 100 \times (\mu_A - \mu_B)/(\mu_A + \mu_B)$ (Figure 1B, insert). (In some simulations I used asymmetrical relations, $\rho_A \neq \rho_B$; see below.) Therefore, at low coherence (small c'), the stimuli to the two groups are similar and hard to distinguish (Figure 1B, bottom). Nevertheless, the competition between the two neural groups will eventually lead to one of the two attractor states, in which one neural group shows elevated persistent activity while the other neural group's activity is suppressed. Such an attractor state is sustained by recurrent network dynamics, and thus it will outlast the stimulus and persist during a mnemonic delay period. If neural group A (or B) wins the competition, the model's decision choice is said to be A (or B).

In computer simulations of the delayed visual discrimination experiment, input presentation (1 s) is followed by a delay period (2 s); the generation of saccadic motor response is not explicitly modeled. Figure 2 shows typical network behavior at three levels of input coherence ($c' = 0\%$, 12.8%, and 51.2%). In all three examples, the neural activity in group A (left) is distinctly higher than that in group B (right), hence the network's decision choice is A (by convention, $\mu_A \geq \mu_B$, so A is the correct choice for any $c' > 0\%$). The neural firing patterns in Figure 2 are notable in several respects, all of which are salient features of decision-correlated neural activity observed in LIP (Shadlen and Newsome, 2001). First, there is a slow time course of activity in pyramidal subpopulation A which, at low coherence, ramps up linearly for the entire stimulation period of 1 s. The ramping slope is steeper at a higher coherence, consistent with the idea that the network accumulates evidence about the input at a faster rate when the signal is stronger. Second, in all three cases, including the one with zero coherence, the firing patterns of the two pyramidal neural groups diverge dramatically over time during the stimulation. This subserves a neural basis for a binary decision to be formed by the network. The winner-take-all competition is a result of the recruitment of feedback inhibition, which develops in parallel with the ramping activity of the inhibitory neurons (bottom). Third, the elevated activity in group A outlasts the transient stimulus and persists through the mnemonic delay period. Further-

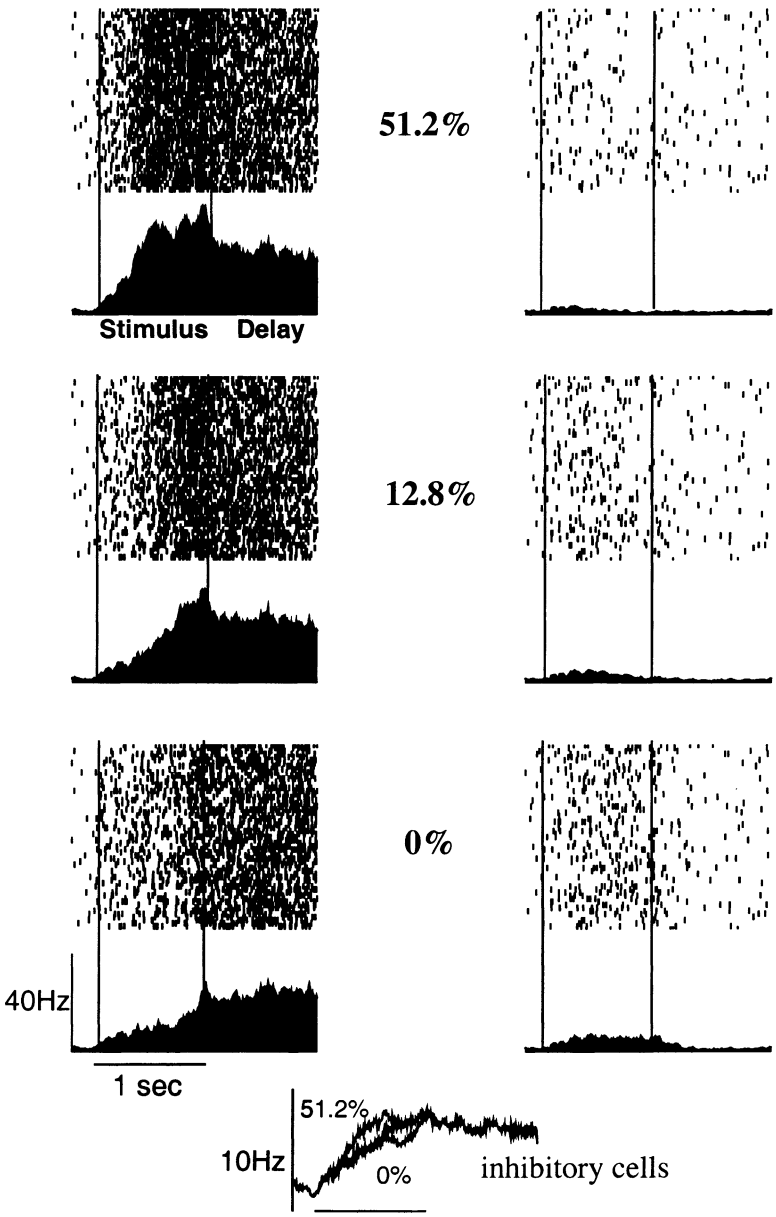

Figure 2. Model Reproduces Salient Characteristics of Decision-Correlated Neural Activity in LIP

Left, neurons in group A; right, neurons in group B. Three trials are displayed with the signal's coherence $c' = 0\%$ (bottom), 12.8% (middle), and 51.2% (top). In all three cases, the attractor A wins the competition and therefore the network's choice is said to be A (correct decision for $c' > 0\%$). Similar to the neural data from LIP, there is a slow time course of activity in group A, with the ramping slope increasing with the signal strength. Moreover, even when the coherence is zero, the firing patterns of the two neural groups diverge dramatically over time during the stimulation, leading to a categorical (binary) decision formed by the network. The inhibitory population, which does not receive direct stimulation but is recruited by pyramidal cells, also shows ramping activity (bottom), and the winner-take-all competition results from this feedback inhibition. Finally, the persistent activity in group A during the mnemonic delay period, with a level independent of the stimulus strength, stores the short-term memory of the decision choice ($\sigma = 4$ Hz).

more, during the delay period, the attractor dynamics is self-sustained and independent of the transient stimulus; hence the persistent activity level is insensitive to the input coherence (and the binary nature of decision choice is preserved). The decision choice is stored in working memory and can be retrieved later to guide a behavioral response.

Neuronal "Coin Tossing" with Inputs of Zero Coherence

At zero coherence, the model network makes decisions randomly (Figure 3). For both examples shown in Figure 3A, the input to group A (red) is slightly larger at the beginning of the stimulation. However, the network does not immediately "latch onto" attractor A. Instead, the two population firing rates (r_A and r_B) remain comparable during the initial phase of stimulation (for several hundreds of milliseconds). Eventually, a decision process transpires that results in a dramatic divergence of the two neural population activities. Attractor A wins the competition in the first trial (left), whereas attractor B wins in the second trial (right).

An interesting way to visualize the decision-making dynamics is to plot the two population firing rates r_A and r_B against each other in a "decision space" (Figure 3B). The network starts with a random walk along the diagonal line ($r_A \cong r_B$) in the decision space, corresponding to the initial phase of stimulation when the decision is not yet made (Figure 3B). Then, the trajectory wanders toward one of the two steady states (attractors) in the decision space. If the trajectory converges to attractor A near the x axis ($r_A \cong 20$ Hz, $r_B \cong 3$ Hz), the network is said to have reached the categorical choice A, whereas if the network converges to attractor B near the y axis ($r_A \cong 3$ Hz, $r_B \cong 20$ Hz), the network's choice is B. When the model was simulated with many trials (n = 1000),

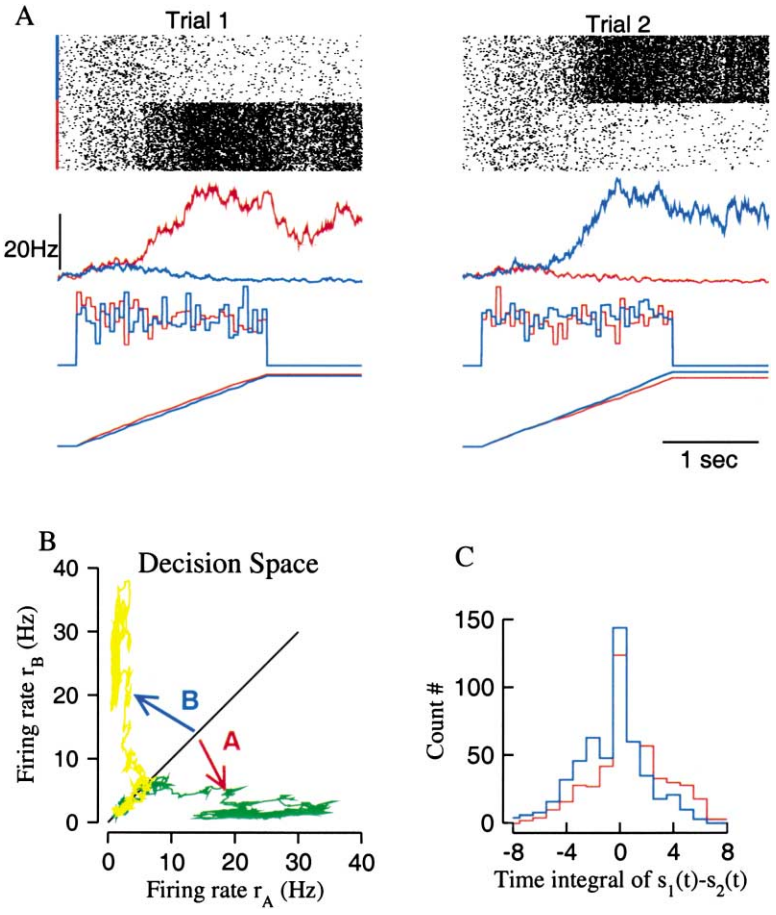

Figure 3. Decision Dynamics with Inputs of Zero Coherence

(A) Two trial simulations (red, neural group A; blue, neural group B). From top to bottom: raster, population firing rates r_A and r_B, stochastic inputs, and time integrals of inputs. In these two examples, decision choice (A or B) is correlated with the larger time integral of the input.

(B) Network dynamics in the decision space for the same two trials as in (A). Note the initial random walk along the diagonal line (when the population activity is similar for the two groups); afterwards the network converges to one of the two attractors (at [r_A = 20 Hz, r_B = 3 Hz] and [r_A = 3 Hz, r_B = 20 Hz].

(C) Histogram of the difference in the input time integral for trials in which the decision choice is A (red curve) or B (blue curve). For trials where attractor A wins, the average I standard deviation of ΔS is 0.8 ± 3, whereas for trials where attractor B wins, it is −0.7 ± 3 (n = 1000, σ = 10 Hz, and stimulus duration is 1 s).

the two choices were found in about equal numbers of trials.

If the stimulus strength is the same for the two neural groups, what determines which of the two wins the competition? One possibility is that even if the input distributions are the same, the actual stochastic realizations of stimuli $s_A(t)$ and $s_B(t)$ in a finite time window are not identical. The neural network could perhaps detect the small difference between the two inputs. This difference could be amplified if the inputs are integrated over a long time period T, $\Delta S = \int_0^T (s_A(t) - s_B(t))dt$, the variance of which increases with time as $\sim T$. Indeed, I found that, in trials where attractor A wins, ΔS is positive in average, whereas in trials where attractor B wins, ΔS is negative in average (Figure 3C). However, the two histograms for ΔS are quite broad and overlap considerably. This means that in a large fraction of trials, even if ΔS is negative (respectively positive), attractor A (respectively B) still wins. Therefore, external stimuli cannot be the main source of randomness in the decision-making process of this model. To confirm this conclusion, I simulated the model without stochastic fluctuations in the stimuli (σ = 0, thus $s_A(t) = s_B(t) = const.$). In this case, the network's behavior is essentially unchanged. The network still makes the two choices with equal probability. The reason is that nonspecific background drives (with an overall rate of 2400 Hz) are much larger than the weak information-specific stimuli (<100 Hz), and thus they determine the amount of stochasticity in the network. Our modeling results suggest that the dominant source of variability in the decision-making process resides not in the sensory stimuli but inside the brain, such as Poisson-like afferent inputs from MT neurons to LIP. However, if external inputs to the two neural groups are stochastic and slightly different, the network is capable of accumulating the difference between the two stimuli, so that decision choice is biased by the time integral of this input difference.

Behavioral Performance and Error Trials

Figure 4A shows the model's performance, i.e., percentage of correct choices as a function of coherence level. The data can be fitted by a Weibull function

$$\%\ \text{correct} = 1 - 0.5 \times \exp(-(c'/\alpha)^{\beta}),$$

where the threshold α is defined as the coherence level at which the performance is $1 - 0.5 \times \exp(-1) = 82\%$ correct. For model simulations with a fixed stimulus duration of 2 s, α = 9.2, β = 1.5. These values are comparable to those of measured psychometric functions of well-trained monkeys. For example, in Roitman and Shadlen (2002), the mean threshold is 6% and the mean slope β = 1.7; in Shadlen and Newsome (2001), the mean threshold is 15% and the mean slope β = 1.1. Furthermore, as expected from the above discussion, when noise is absent in the stimulus (σ = 0), the neurometric function is virtually unchanged (α = 8.9, β = 1.5). This

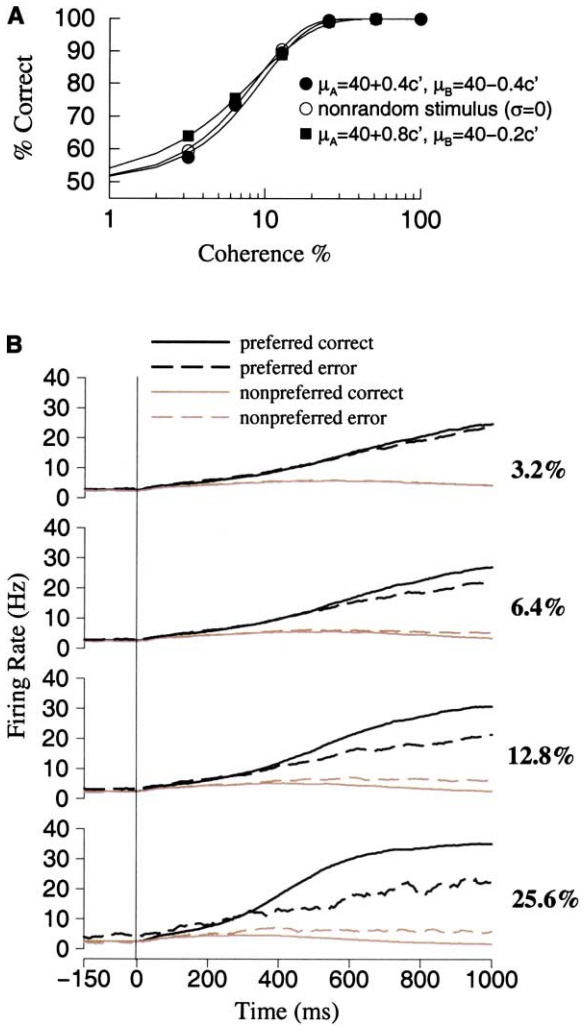

Figure 4. Performance and Population Activity Time Courses

(A) Neurometric functions (% correct). Data are fitted by Weibull functions. Filled circle: noisy stimuli (σ = 4 Hz) with symmetrical dependence of the mean values on input coherence (the ratio of the slopes is $\rho_A/\rho_B = 1$). Open circle: without noise in the stimulus (σ = 0), the network's performance is virtually the same. Filled square: asymmetrical dependence of the mean stimuli on coherence (the ratio of the slopes is $\rho_A/\rho_B = 4$). The coherence threshold is slightly lower.

(B) Time course of population activity for four coherence levels. Black curves, the choice is the preferred stimulus; gray curves, the choice is the nonpreferred stimulus. Correct trials are indicated by solid curves, error trials by dashed curves.

result is consistent, although not directly comparable, with the experimental observation that the trial-to-trial variability in the MT neuronal responses and in the animal's decision choices is essentially the same when the random dot displays vary from trial to trial, or when identical random dot patterns are used (with fixed seed for the random number generator) in different trials (Britten et al., 1996).

I also considered the case when the average signals μ_A and μ_B depend on the coherence c' in an asymmetrical fashion, i.e., the slopes ρ_A and ρ_B are not the same. Assuming that μ_A and μ_B mimic the average MT neural responses for the preferred and null directions, respectively, data suggest that ρ_A/ρ_B can be as large as 4 (Britten et al., 1993). I tested several values of ρ_A while fixing $\rho_B = \rho_A/4$. Figure 4A shows the neurometric function computed with $\rho_A = 0.8$ and $\rho_B = 0.2$, which gives a slightly lower coherence threshold ($\alpha = 8.7$, $\beta = 1.1$). With a larger value of ρ_A, the difference between the two stimuli increases faster with c', and the coherence threshold is lower.

Figure 4B shows the time evolution of neural population response for four coherence levels. In correct trials (solid curves), neural activity increases with time in response to a preferred stimulus. For a nonpreferred stimulus, it first increases slightly (due to direct but smaller external drive), then decreases when the winner-take-all process transpires. The divergence of the two neural groups is faster at higher coherence levels. In error trials (dashed curves), population activity of a neural group increases with time if it wins the competition and hence the decision choice is its preferred stimulus, and decreases when it loses competition. The time courses are virtually identical for correct and error trials at a low coherence level (3.2%). At a higher coherence level, neural activity for the preferred choice is lower in error trials than in correct trials, and the difference becomes increasingly significant with larger stimulus strengths. This is because the winning neural group receives a smaller direct input in error trials than in correct trials. Similarly, when the chosen stimulus is nonpreferred, the losing neural group receives a larger direct input in error trials than in correct trials; hence its activity is somewhat higher in error trials compared to correct trials. These differences between correct and error trials as a function of coherence level have been consistently observed experimentally (Figure 4 in Shadlen and Newsome, 1996; Figure 12 in Shadlen and Newsome, 2001; Figure 7 in Kim and Shadlen, 1999; and Figure 11 in Roitman and Shadlen, 2002).

Reaction Time Simulations

I also used the model to simulate the reaction time experiment, where the animal is allowed to make the behavioral response to indicate its perceptual choice at any time during stimulus viewing (Roitman and Shadlen, 2002). I assumed that in the reaction time paradigm, the decision is reached when either of the two neural groups first reaches a threshold of population activity level (Carpenter, 1981; Schall, 2001). As shown in Figure 5A, at zero or low coherence, neural activities ramp up slowly, so that the mean deliberation or decision time is larger. Moreover, decision time varies considerably from trial to trial (Figure 5A, top left), and the decision time histogram is broad (Figure 5A, bottom left). At high coherence, the decision time is smaller and less variable (Figure 5A, top right), and its histogram is much narrower (Figure 5A, bottom right). It is apparent in Figure 5A that as long as the threshold level is not too small, its precise value is not critical; another choice of threshold (say 18 Hz) would simply yield somewhat different mean and variability of decision times.

The neurometric function from reaction time simulations is displayed in Figure 5B (left), with $\alpha_{RT} = 8.4$, $\beta_{RT} = 1.6$. The coherence threshold is indistinguishable from

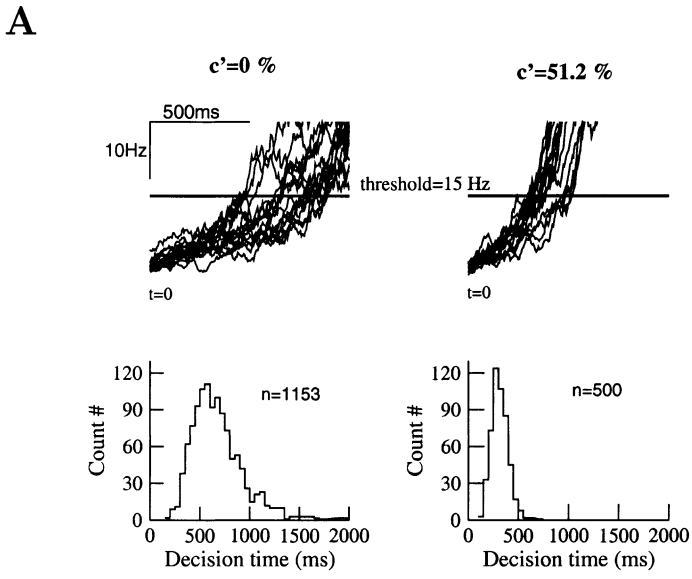

Figure 5. Reaction Time Simulations

Same parameters as in Figure 4.

(A) During a 2 s stimulation, at the moment when one of the two neural groups reaches a fixed threshold (15 Hz) of population firing activity, the decision is made and the deliberation or decision time is read out. The decision time is longer and more variable at low coherence (left) than at high coherence (right). This is further quantified by the decision time histogram (bottom), which has a larger mean and is broader at low coherence (left) than at high coherence (right).

(B) Left: Neurometric functions for the reaction time stimulation (circle) and with fixed stimulus duration of 1 s (square). The coherence threshold (defined by 82% correct) is $\alpha_{RT} = 8.4\%$ and $\alpha_{FD} = 10.4\%$. Right: Average decision time is linear in the logarithm of the coherence level, ranging from 200 ms at high c' to 800 ms at low c'. At very low coherence there is a saturation. Note the large standard deviation of decision time, especially at low coherence.

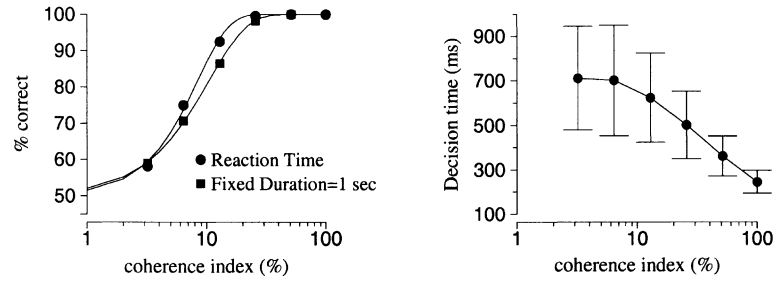

that obtained in simulations with fixed stimulus duration of 2 s (Figure 4A). This is because, with a sufficiently high threshold (15 Hz in Figure 5), reaching that firing threshold virtually guarantees that the corresponding attractor wins. However, it is slightly lower than the coherence threshold $\alpha_{FD} = 10.4$ obtained from stimulations with fixed stimulus duration of 1 s (Figure 5B, left). The ratio $\alpha_{RT}/\alpha_{FD} \cong 0.8$, in agreement with the experimental observations (Roitman and Shadlen, 2002). It was suggested that the discrepancy can be explained if at zero or low coherence reaction time is often longer than 1 s, and hence the network has more time to form a decision in the reaction-time task (Roitman and Shadlen, 2002). This is indeed the case for the present model (Figure 5A, left).

The mean decision time varies linearly with the logarithm of the signal strength from 200 ms at high coherence to 800 ms at low coherence, and it saturates as coherence goes to zero (Figure 5B). (Note also the large standard deviation of decision times, especially at low coherence.) This is in agreement with Roitman and Shadlen (2002), who reported a linear relationship between the average reaction time and the logarithm of the coherence level. In that experiment, the animal's trial-averaged reaction time ranges from 300 ms at high coherence to 900 ms at low coherence. The extra 100 ms compared to the model can be easily accounted for in the intact animal, by the latency for the signal to reach LIP and the response time within the saccadic generation system. Moreover, decision times in the model can be increased or decreased by changing parameters such as the recurrent connection strength w_+ (see below) and the mean stimulus amplitude μ_0 (data not shown).

Dependence on Time Integration of Long Stimulus Signal

Better performance in reaction-time simulations than with fixed 1 s stimuli indicates that long stimulus presentation is important for the decision process. In visual motion discrimination experiments, it was found that the coherence threshold increases, and the animal's performance deteriorates, steeply with decreased stimulus duration (Britten et al., 1992). I tested directly the importance of time integration in simulations where the stimulus duration was varied systematically from trial to trial. The stimulus offset was followed by a fixed delay of 2 s and the decision choice was made according to which of the two attractors wins the competition. When the stimulus is very short (say 200 ms), in many trials

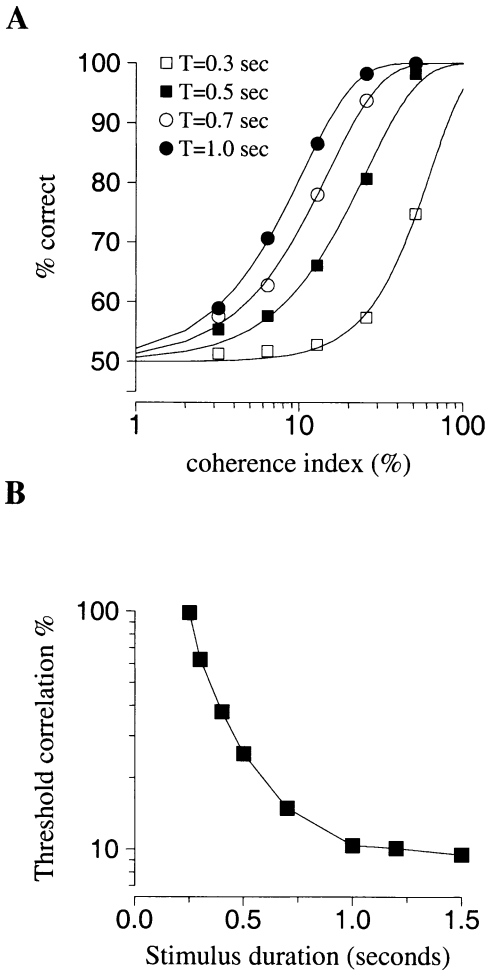

Figure 6. Dependence of the Decision Performance on the Duration of Stimulus Presentation

The stimulus offset is followed by a fixed delay of 2 s, and the decision choice is based on which of the two attractors wins the competition.

(A) Neurometric function is shifted to the left with longer stimuli.

(B) Coherence threshold (α defined by 82% correct choices) decreases with the stimulus duration and plateaus for stimulus presentation longer than 1.5 s.

none of the attractors could be reached, and the network reverted back to the resting state after the stimulus. In that case the choice was assigned randomly. I found that, in agreement with the behavioral data, the neurometric function of the network model shifts to the left with increasing stimulus duration (Figure 6A). The coherence threshold decreases dramatically as the stimulus duration is varied from 200 ms to 1 s, then further decreases gradually and plateaus for stimulus durations larger than 1.5 s (Figure 6B). This result provides a direct demonstration that decision-making behavior of the model critically depends on time integration over a long stimulus presentation.

Slow Reverberation Mediated by NMDA Receptors

In the model, the biophysical properties and neurons and synapses were calibrated by experimental measurements, with typical time constants from a few to tens of milliseconds. The longest time constant is that of decay for NMDA receptor-mediated synaptic current ($\tau_{NMDA} = 100$ ms). What, then, allows the model network to carry out time integration for more than one second? I found that the neural integration is a network phenomenon, subserved by strong synaptic excitatory reverberations. This can be shown by reducing recurrent connections within each of the two neural assemblies so that attractor dynamics of persistent activity is lost (Figure 7A). In this case, all the three salient features of a decision-making network are destroyed. First, there is much less ramping activity (stimulus integration), which is now limited to about 200–300 ms. Second, at low coherence the firing activities of the two neural groups cannot be distinguished, and therefore a categorical decision is not possible. Third, there is no persistent activity during the delay period, and hence no short-term memory storage.

On the other hand, it is important that synaptic reverberation be sufficiently slow. With an increased strength of recurrent connections, synaptic reverberation is more powerful and faster, and the persistent firing rate during the delay period is twice as high (40 Hz) as in control (20 Hz) (Figure 7B, left). In this case, the network's performance is significantly worse (Figure 7B, right). Therefore, there is an optimal range of recurrent connection strength, below and above which the network's integration time is shortened and decision-making performance deteriorates accordingly.

Slow reverberation depends on the assumption that recurrent excitation is primarily mediated by the slow NMDA receptors. In the contrasting case where there are only fast AMPA receptors (time constant less than 5 ms) at recurrent synapses, the network can still show attractor dynamics. However, the network cannot integrate stimuli for more than tens of milliseconds, and it "latches onto" one of the two attractors immediately after the stimulus onset (data not shown). Therefore, slow synaptic excitation mediated by NMDA receptors is more suitable for subserving time integration of inputs in a decision-making neural network. I will come back to this point in the Discussion.

Decision Reversal

I showed that slow stimulus integration (subserved by ramping neural activity) is important for the network's decision-making performance. Can the model network subtract negative signals as well as accumulate positive signals, as a true neural integrator is expected to do? To answer this question, I assessed how the model's decision process is altered when the input signal is reversed during stimulation. Figure 8A shows the network's behavior in the case when the initial and reversed signals have the same strength (c' is switched from 6.4% to −6.4%). In the control case, the decision choice is A in 72% of the trials. In signal reversal, the input is initially larger for group A, and becomes larger for group B after signal switch. It was found that the impact of signal switch critically depends on the timing of reversal. If reversal happens at the beginning of the stimulus presentation, it is the same as exchanging the two stimuli. The decision choice is 28% for A (and 72% for B),

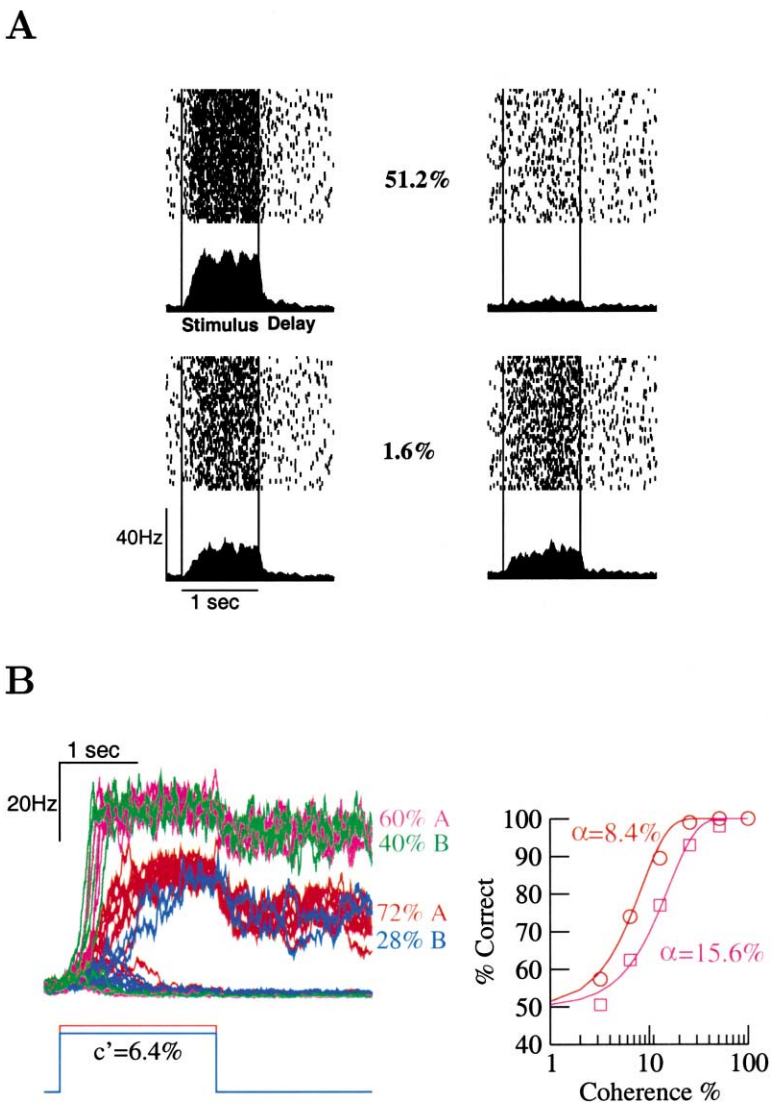

Figure 7. Optimal Decision-Making Performance Requires Sufficiently Strong and Slow Synaptic Reverberations

(A) When the strength of recurrent connections is weaker ($w_+ = 1.4$ instead of $w_+ = 1.7$), attractor dynamics can no longer be sustained by intrinsic network excitation. Neural activities of subpopulation A (left) and B (right) are shown at two coherence levels (1.6% and 51.2%). Same conventions as in Figure 2. In this case, there is a reduced time integration (ramping activity), categorical choice at low coherence is lost, and mnemonic persistent activity is absent during the delay period.

(B) Network behavior with an increased strength of recurrent connections ($w_+ = 1.8$). Left: population activities in ten individual trials for the control (red, neural group A; blue, neural group B) and for enhanced recurrency (purple, neural group A; green, neural group B). With stronger excitatory reverberations, persistent activity level is doubled (from 20 Hz in control to 40 Hz), and the integration time of stimulus is shortened by a half. The performance is reduced from 72% to 60% correct at $c' = 6.4\%$. Right: the network's performance is worse, with the neurometric function's threshold increased from 8.4% (red) to 15.6% (purple).

as expected. With an increasing time of reversal, up to about 600–700 ms, the percentage choice for A increases linearly, consistent with a pure integration where evidence for A is added and evidence for B is subtracted in neural group A (and the opposite process takes place in neural group B). However, if the reversal occurs too late (>700 ms), its impact becomes negligible. The percentage choice for A plateaus at 72%, the same level as in control, as if the signal reversal did not take place at all. Note that the onset of saturation roughly corresponds to the average decision time (700 ms); when the population activity of a neural group (A or B) has reached a threshold, the network settles in an attractor state, and intrinsic recurrent inputs become dominant over the weak external inputs. This result clearly demonstrates the two steps of a decision-making process in the model: initial integration of inputs by ramping neural activity and categorical decision choice by the attractor dynamics.

Can a decision still be reversed late in time in spite of attractor dynamics? One can argue that the answer should be yes, if the new stimulus (after signal reversal) is sufficiently strong. Figure 8B shows the network's behavior with signal reversal at time $t = 1$ s in the middle of a 2 s stimulation, as a function of the reversed signal's coherence level. With increasing strength of the reversed signal, the % choice for A decreases, and the % choice for B increases, linearly in a graded manner. However, at the coherence level of about 70%, there is an abrupt transition, beyond which the % choice for A goes to zero. In other words, when the reversed signal's coherence is larger than 70%–80%, the second external stimulus is powerful enough to overcome the intrinsic attractor dynamics so that the decision is reversed in favor of the new (stronger) evidence. Figure 8C shows the time course of population activities of group A (red) and group B (blue) in the control (top) and with signal reversal (bottom). During the process of decision reversal, there is a slow ramping down of neural activity in group A, and a slow ramping up of neural activity in group B, over several seconds. Therefore, convergence to an attractor state does not mean that the network is

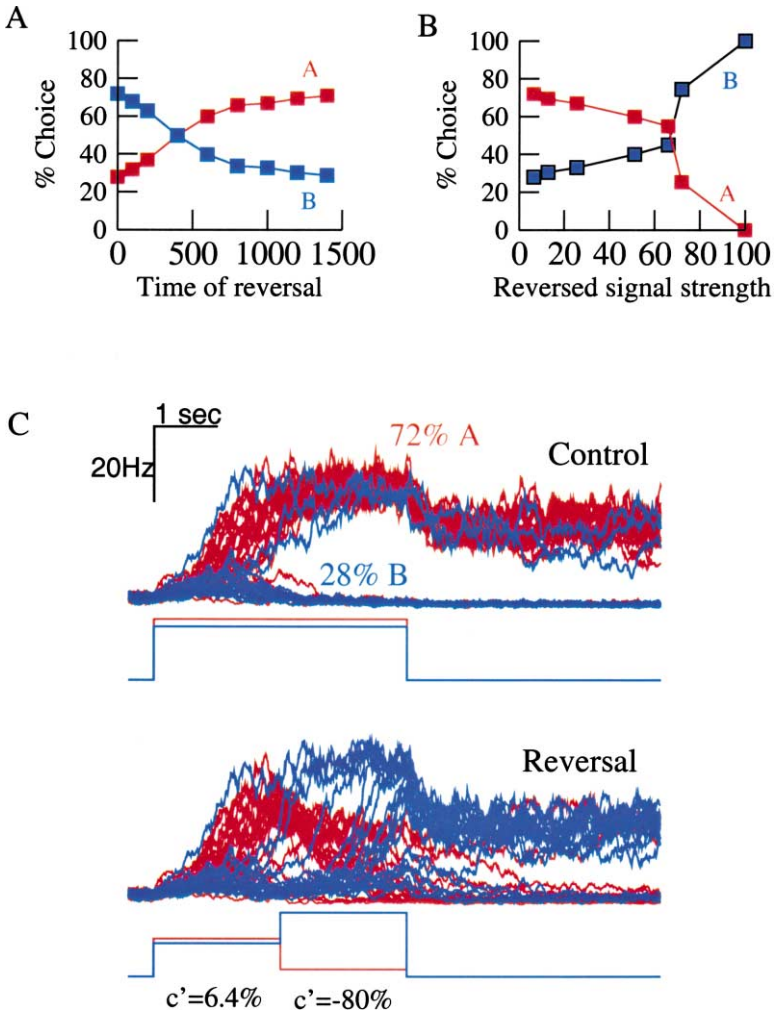

Figure 8. Decision Reversal

(A) The input signal is reversed during stimulation, where the signal strength is weak (6.4%) and the same before and after the reversal. Percentage choices for A and B as function of the onset time of reversal. The dependence is initially linear as a function of the time of reversal, consistent with an integration of the first and second inputs of the opposite signs. However, the behavioral performance is no longer affected if signal reversal occurs too late (e.g., the reversal time is larger than 700 ms after the stimulus onset), when the network becomes dominated by the intrinsic attractor dynamics.

(B) Even when the signal is reversed 1 s after the stimulus onset, the decision is still reversable by a more powerful input. Percentage choices for A and B as function of the coherence level of the reversed signal. When the new input is sufficiently large (coherence above 70%–80%), the decision is always reversed in favor of the "new evidence."

(C) Examples for control (top) and signal reversal from $c' = 6.4\%$ to -80% at 1 s after the stimulus onset (bottom). Note the slow ramp-down of population activity in group A (red), and ramp-up of population activity in group B (blue) during the second half of the stimulation when the decision is reversed.

totally locked; attractor network dynamics is capable of decision reversal based on the amount of evidence for the two alternative signals.

Discussion

Cortical Basis for Making Perceptual Decisions

Decision making holds the key to our understanding of how neural processes in the brain link sensory stimulus to psychophysical choice and action. This is a major topic of research in cognitive psychology (see Luce, 1986; Hastie, 2001, for reviews). In recent years, this field has begun to attract attention of physiologists interested in the neural basis of decision making (Parker and Newsome, 1998; Platt and Glimcher, 1999; Romo and Salinas, 2000; Schall, 2001). Decision-related neural activities have been found in association cortices, such as posterior parietal (Shadlen and Newsome, 1996, 2001), dorsal prefrontal (Kim and Shadlen, 1999; Quintana and Fuster, 1992, 1999), and premotor (Romo et al., 1997; Hernández et al., 2002) areas. In the same cortical circuits, persistent neural activity is commonly observed during the delay of working memory tasks. This may not be a mere coincidence. On the one hand, recurrent attractor networks represent a leading candidate mechanism to account for mnemonic persistent neural activity (Amit, 1995; Wang, 2001). On the other hand, attractor networks seem a natural modus operandi for winner-take-all competition leading to a categorical choice. Winner-take-all (Hertz et al., 1991) has been discussed previously in such contexts as competitive learning or selective attention. Here, I showed that it can also subserve perceptual discrimination in an attractor network of spiking neurons. However, attractor models do not seem to easily account for the buildup of neural activity (Schall et al., 1995; Shadlen and Newsome, 1996, 2001), the presumed neural process underlying slow accumulation of sensory evidence. Indeed, previous recurrent network models are typically characterized by extremely fast responses to inputs (Tsodyks and Sejnowski, 1995; van Vreeswijk and Sompolinsky, 1998). Slow temporal integration and categorical choice are two indispensable aspects of a decision process, which seem to be difficult to be accomplished by a single network. In principle, these two steps could be done sequentially by different cortical areas. However, neural correlates of both processes are usually observed in the same cortical area (Shadlen and Newsome, 2001; Roitman and

Shadlen, 2002; Hernández et al., 2002), suggesting that they may take place within a local cortical network.

A Slow Reverberation Theory of Decision Making

In this paper, I presented an attractor model for perceptual decision making which, by virtue of slow reverberation mediated by NMDA receptors, is capable of both time integration and categorical decision formation. The model is biophysically realistic, built on the known physiology of cortical neurons and synapses. I showed that this recurrent network model reproduces characteristic behaviors of LIP single neurons during a visual discrimination experiment (Shadlen and Newsome, 1996, 2001; Roitman and Shadlen, 2002), including (1) neural activity is primarily correlated with the decision choice and not the signal (when stimulus coherence is zero); (2) spike discharges build up over time, at a faster speed with stronger stimulus strength; (3) at low coherence, neuronal responses are the same in correct and error trials, but at high coherence, neurons signal the categorical choice more weakly in error trials than in correct trials; and (4) categorical choice is stored in working memory during the delay period in the form of binary activity patterns that are independent of the stimulus coherence. The model also yields behavioral performance and reaction times comparable to the data from behaving animals: (1) the Weibull neurometric function has a coherence threshold of about 10% and a slope close to 1; (2) coherence threshold decreases with integration time, from more than 50% for stimuli of 250 ms to less than 10% for stimuli lasting for 2 s; and (3) mean deliberation or decision time decreases linearly with the logarithm of the stimulus coherence.

Certain aspects of experimental data have not been duplicated by the model. In parietal and prefrontal neurons, at high coherence levels, if the choice is the preferred direction of recorded cells, neural activity is much smaller in error trials than in correct trials, whereas if the choice is the null direction, neural activity is somewhat larger in error trials than in correct trials (Shadlen and Newsome, 1996, 2001; Kim and Shadlen, 1999; Roitman and Shadlen, 2002). The model does exhibit this phenomemon and suggests an explanation for it (Figure 4B), but the effect is more limited in the model than in real neurons. It is unclear whether a better quantitative match can be achieved by appropriately adjusting model parameters. Moreover, I have not attempted to accurately reproduce the measured distributions of reaction times for correct and error trials. This issue deserves to be analyzed in detail and is beyond the scope of the present paper.

Comparison with the Diffusion Model

The attractor model is to be contrasted with accumulator or counter models commonly used in psychology (Ratcliff, 1978; Ratcliff et al., 1999; Luce, 1986). A similar model was proposed to describe the neural process in LIP for the visual motion discrimination experiment (Ditterich et al., 2001). According to this "integrate-and-decide" model, an LIP neuron selective to the left direction (L) integrates the input s_L plus random noise, in the sense of mathematical calculus, so that its firing activity r_L is described by $dr_L/dt = s_L + \text{noise}$. Similarly, a competing neuron selective to the right direction (R) is described by $dr_R/dt = s_R + \text{noise}$. Consequently, the difference $X = r_L - r_R$ obeys the equation

$$\frac{dX}{dt} = s_L - s_R + \text{noise}, \quad X(t) = (s_L - s_R)t + \int_0^t dt\ \text{noise}$$

$X(t)$ undergoes a random walk in real time (a diffusion process), biased by a constant ramp $(s_L - s_R)t$ (the rate of accumulation $(s_L - s_R)$ increases with the signal strength, $s_L = s_R$ for zero strength). When $X(t)$ reaches a prescribed threshold θ (respectively $-\theta$), decision is reached for choice L (respectively choice R), and the reaction time $RT = t$ is registered. The model for the saccade generation system proposed by Carpenter (Carpenter, 1981; Carpenter and Williams, 1995; Reddi and Carpenter, 2000) is similar in spirit, with an emphasis on the assumption that the rate of linear accumulation fluctuates randomly from trial to trial.

The diffusion model is intuitively appealing and has been used to fit psychophysical data. However, it is unclear how several critical features of the diffusion model can be implemented in a biophysically realistic neural network. First, the mechanism for the presumed subtraction operation is not specified. In the biophysical model, competition is realized by feedback inhibition between the two neural groups (see also Usher and McClelland, 2001), which effectively provides a mechanism for input subtraction. Second, in the diffusion model, the decision is made by reaching a preset firing threshold and there is no memory of a categorical choice. Additional ingredients must be incorporated into the model in order to account for a delayed discrimination experiment such as that of Shadlen and Newsome (2001). By contrast, in my model both categorical decision and memory store are naturally accomplished by the attractor dynamics. Third, there is no explanation as to the source of noise. In the present model, noise is primarily due to stochastic background inputs inside the brain, rather than external stimuli, in agreement with the experimental evidence (Britten et al., 1996). Finally, the diffusion model assumes that the characteristic time constant of the system is infinite, which is biologically unrealistic. This last point has been the focus of a recent work (Usher and McClelland, 2001) where a leakage is added so that the model's time constant τ becomes finite. The "leaky integrate-and-decide" model becomes

$$\frac{dX}{dt} = -\frac{X}{\tau} + s_L - s_R + \text{noise}$$

This model can only integrate the input over a time span limited by τ. Thus, τ must be hundreds of milliseconds, if not longer, in order for the model to reproduce the long accumulation process observed experimentally. Such a long time constant cannot be directly related to fast glutamatergic excitatory synaptic transmission mediated by AMPA receptors ($\tau_{syn} \cong$ 1–3 ms) and NMDA receptors ($\tau_{syn} \cong$ 50–100 ms). Here, it is proposed that a long integration time constant can be achieved biophysically in a realistic cortical network, by a combination of slow synapses dominated by NMDA receptors and strong network recurrency. Indeed, recurrent excitation implies an additional term in the equation,

$$\frac{dX}{dt} = \frac{(-X + w_{syn}X)}{\tau_{syn}} + s_L - s_R + \text{noise}$$

where τ_{syn} is the synaptic time constant and w_{syn} is the strength of excitatory recurrency. As a result, the effective time constant of the model is given by $\tau_{eff} = \tau_{syn}/(1 - w_{syn})$ (Seung, 1996; Wang, 2001). As is clear from this formula, the larger are τ_{syn} and w_{syn}, the longer is τ_{eff}. For instance, if $\tau_{syn} = 100$ ms and $1 - w_{syn} = 0.05$, then $\tau_{eff} = 2$ s. (When w_{syn} is too large, ≥ 1, this linear model is no longer valid and nonlinearity of the biophysical model must be taken into account.)

Integration Time and Robustness of Decision-Making Networks

In model simulations, I have shown that integration time is shorter if excitatory recurrency is too weak (below a critical level) to sustain attractor dynamics (Figure 7A). On the other hand, the integration time also decreases with too strong recurrent excitatory connections (Figure 7B). Therefore, the reverberation model with varying degrees of recurrent connections is capable of generating a spectrum of integration times, which may be desirable for different cortical circuits dedicated to specific computations. For instance, even if recurrent interactions are not strong enough to sustain attractor dynamics, excitatory reverberations can still be significant and capable of integrating stimulus signals for 100–300 ms, which may be all that is needed in certain cortical areas (Schall, 2001; Krauzlis and Dill, 2002; Cook and Maunsell, 2002). On the other hand, strongly reverberatory attractor networks could be relevant to other areas that are involved less in accumulating sensory evidence and more in selecting an action or storing a decision choice in working memory.

The above discussion indicates that in order to achieve the longest accumulation time possible, the network recurrency needs to be above but close to the onset of attractor dynamics, or near the bifurcation of the persistent activity states. This implies a certain amount of parameter tuning and raises the question of the robustness of this decision-making network. In computer simulations I did not find it necessary to precisely adjust model parameters. In fact, most of the parameters used here are identical to those in Brunel and Wang (2001). The network model may not require the same degree of fine-tuning of parameters as, for example, the line attractor model of oculomotor neural integrator (Seung, 1996; Seung et al., 2000). A major difference is that the present model has a discrete number of (two, potentially several) attractor states, whereas the oculomotor integrator model has a (quasi-)continuum of attractor states whose realization is much subtler and more sensitive to parameter mistuning.

On the other hand, chance-level performance at zero coherence requires the two halves of the network to be perfectly symmetrical. This is generally true: the outcome of coin-tossing cannot be 50-50 if the coin is biased. Similarly, the widely used diffusion model of decision-making will not yield 50-50 performance if the input is not symmetrical. I have assessed the effect of symmetry breaking on the attractor model performance. The recurrent synapses within each of the two neural assemblies are proportional to the parameter w_+ (see Experimental Procedures). I have fixed the value of $w_+ = 1.8$ in neural group A and reduced its value in neural group B by a small percent ρ. I found that with $\rho = 1\%, 2\%, 4\%, 5\%$, the recurrent excitation with group B gradually weakens. As a consequence, the firing rate of the persistent state in group B is decreased linearly from $r_B = r_A = 42$ Hz to $r_B = 39, 36, 28, 24$ Hz, respectively. Thus, the resulting asymmetry in the neural activity is quite large, $(r_A - r_B) = 18$ Hz or $(r_A - r_B)/r_A = 18/42 = 43\%$ with $\rho = 5\%$.

The percentage response for A can be fitted by % correct $= 1 - \epsilon \times \exp(-(c'/\alpha)^{\beta})$ and is $(1 - \epsilon)$ at zero coherence. I found that $(1 - \epsilon) = 50\%, 53\%, 62\%, 70\%, 74\%$ for $\rho = 0\%, 1\%, 2\%, 4\%, 5\%$, respectively. The other parameters α and β change only modestely. Therefore, the change is gradual, not abrupt or discontinuous, with increasing ρ. In this sense the network model is reasonably robust. Note that 74% response for one of the two choices deviates significantly from chance-level performance. However, this occurs with a large amount of functional asymmetry (the difference in the two persistent rates is 18 Hz, 43% from control). It is difficult to imagine any model that would still give close to 50-50 performance with such a large functional asymmetry. This begs the question: how can symmetry (or homogeneity in general) be realized in a cortical circuit? One possibility is that asymmetry or heterogeneity could be reduced or eliminated by activity-dependent mechanisms, such as homeostatic synaptic scaling (Turrigiano, 1999). Indeed, in a separate study, we show that synaptic scaling can effectively homogenize a working memory network, so that the long-term firing rates of different neural groups are regulated to be similar in spite of network heterogeneities (A. Renart et al., submitted).

Experimental Tests

The present model can be tested experimentally at two different levels. At the cellular level, the model suggests a critical role of NMDA receptors in cortical decision-making circuits. Interestingly, immunochemical studies show that the mRNA expression of NMDA receptors is much higher in parietal and prefrontal cortices (putative foci of decision) compared to primary visual cortex (an early sensory area) of the human brain (Scherzer et al., 1998). It would be of interest to physiologically assess NMDAR-mediated synaptic transmission at intrinsic synapses of parietal and prefrontal cortices and its role in decision making of behaving animals. Moreover, slow reverberation could also be subserved by other biophysical mechanisms, such as slow synaptic facilitation or slow ionic channels in single neurons. On the other hand, the attractor model for decision making remains to be tested experimentally with behaving animals. In particular, the model suggests that signal reversal could be a useful tool to test the attractor model, whose predictions both for the behavioral performance and for the neural activity correlated with decision reversal (Figure 8) are different from those by the diffusion model of linear integration. However, such manipulations need to be carefully designed, since the effect of stimulus reversal on an animal's performance would be completely differ-

ent depending on the way the animal is trained and rewarded.

It is likely that a quantitative comparison between the model and the experiments requires refinements and extension of this model. For example, here I used a simple model to simulate a two-choice paradigm. However, in visual discrimination, the motion direction is not necessarily binary but can be any angle between 0 and 360 degrees. It will be interesting to investigate the decision-making process in a recurrent network model that can encode any direction as an analog quantity, by virtue of a continuum of attractor states (spatially localized persistent firing patterns) (Compte et al., 2000). Moreover, the model could be extended to include a reciprocal loop between a decision area (such as LIP) and a sensory area (MT). MT is known to encode motion signal from which the decision choice is derived (Newsome et al., 1989; Salzman et al., 1990; Britten et al., 1992; Bisley et al., 2001; Dodd et al., 2001). In the present work, we focused on the decision network and assumed a very simple form of stimulus encoding by MT neurons. In future work, it will be interesting to consider in more detail how motion stimuli are represented in MT via the distribution of correlated neuronal responses (Zohary et al., 1994; Shadlen et al., 1996; Simoncelli and Heeger, 1998). Moreover, MT activity shows a significant choice probability (Britten et al., 1996) that can be large with certain types of visual motion stimulus (Dodd et al., 2001). However, it is unclear whether this is a reflection of top-down modulation from a decision area such as LIP. Finally, decisions depend on prior experience and expected reward (Platt and Glimcher, 1999; Gold and Shadlen, 2001; Platt, 2002; see also special issue of *Neuron* on Reward and Decision, October, 2002), but the underlying neural mechanisms are unknown and remain to be investigated. Experimental and modeling work along these lines will help to elucidate the cellular and synaptic basis of the decision-making process in the brain.

To conclude, the present work supports the view that cortical areas endowed with persistent activity are functionally not limited to short-term memory storage. The concept of slow reverberation may be a key to understanding their computational roles in cognition.

Experimental Procedures

The Cortical Network Model

The model combines a network architecture taken from Amit and Brunel (1997) and descriptions of synaptic currents from Wang (1999). The network is composed of N neurons, with N_E pyramidal cells (80%) and N_I interneurons (20%) (Braitenberg and Schütz, 1991). It represents a local cortical circuit in the posterior parietal cortex. For the sake of clarity, I have used the simplest version of the model, with the assumption that the network encodes two stimulus directions (left or right). Each stimulus activates a distinct and small subpopulation of fN_E excitatory cells ($f = 0.15$). The remaining $(1 - 2f)N_E$ neurons do not respond to either of the stimuli. This is a simple realization of the common experimental protocol, where the physiological measurements are done with the best and worst stimuli (preferred and null directions) of the recorded cell. Simulations reported in this paper were done with $N_E = 1600$, $N_I = 400$.

Neurons

Both pyramidal cells and interneurons are described by leaky integrate-and-fire neurons (see for example Tuckwell, 1988) and are characterized by a resting potential $V_L = -70$ mV, a firing threshold $V_{th} = -50$ mV, a reset potential $V_{reset} = -55$ mV, a membrane capacitance $C_m = 0.5$ nF for pyramidal cells and 0.2 nF for interneurons, a membrane leak conductance $g_L = 25$ nS for pyramidal cells and 20 nS for interneurons, and a refractory period $\tau_{ref} = 2$ ms for pyramidal cells and 1 ms for interneurons. The corresponding membrane time constants are $\tau_m = C_m/g_L = 20$ ms for excitatory cells and 10 ms for interneurons (McCormick et al., 1985). Below threshold, the membrane potential $V(t)$ of a cell

$$C_m \frac{dV(t)}{dt} = -g_L(V(t) - V_L) - I_{syn}(t),$$

where $I_{syn}(t)$ represents the total synaptic current flowing into the cell.

Synapses

The network is endowed with pyramid-to-pyramid, pyramid-to-interneuron, interneuron-to-pyramid, and interneuron-to-interneuron connections (Figure 1A). Recurrent excitatory postsynaptic currents (EPSCs) have two components mediated by AMPA and NMDA receptors, respectively. External synaptic inputs send to the network all the information (stimuli) received from the outside world, as well as background noise due to spontaneous activity outside the local network. In simulations, external EPSCs were mediated exclusively by AMPA receptors. The total synaptic currents are given by

$$I_{syn}(t) = I_{ext,AMPA}(t) + I_{rec,AMPA}(t) + I_{rec,NMDA}(t) + I_{rec,GABA}(t)$$

in which

$$I_{\text{ext,AMPA}}(t) = g_{\text{ext,AMPA}}\,(V(t) - V_E)\, s^{\text{ext,AMPA}}\,(t)$$

$$I_{\text{rec,AMPA}}\,(t) = g_{\text{rec,AMPA}}\,(V(t) - V_E) \sum_{j=1}^{C_E} w_j s_j^{\text{AMPA}}\,(t)$$

$$I_{\text{rec,NMDA}}(t) = \frac{g_{\text{NMDA}}(V(t) - V_E)}{(1 + [\text{Mg}^{2+}]\,\exp(-0.062V(t))/3.57)} \sum_{j=1}^{C_E} w_j s_j^{\text{NMDA}}\,(t)$$

$$I_{\text{rec,GABA}}(t) = g_{\text{GABA}}\,(V(t) - V_I) \sum_{j=1}^{C_I} s_j^{\text{GABA}}\,(t)$$

where $V_E = 0$ mV, $V_I = -70$ mV. The dimensionless weights w_j represent the structured excitatory recurrent connections (see below), the sum over j represents a sum over the synapses formed by presynaptic neurons j. NMDA currents have a voltage dependence that is controlled by extracellular magnesium concentration (Jahr and Stevens, 1990), $[\text{Mg}^{2+}] = 1$ mM. The gating variables, or fraction of open channels s, are described as follows. The AMPA (external and recurrent) channels are described by

$$\frac{ds_j^{\text{AMPA}}\,(t)}{dt} = -\frac{s_j^{\text{AMPA}}\,(t)}{\tau_{\text{AMPA}}} + \sum_k \delta(t - t_j^k)$$

where the decay time of AMPA currents is taken to be $\tau_{AMPA} = 2$ ms (Hestrin et al., 1990; Spruston et al., 1995), and the sum over k represents a sum over spikes emitted by presynaptic neuron j. In the case of external AMPA currents, the spikes are emitted according to a Poisson process with rate $\nu_{ext} = 2.4$ kHz independently from cell to cell. NMDA channels are described by

$$\frac{ds_j^{\text{NMDA}}\,(t)}{dt} = -\frac{s_j^{\text{NMDA}}\,(t)}{\tau_{\text{NMDA,decay}}} + \alpha x_j(t)(1 - s_j^{\text{NMDA}}\,(t))$$

$$\frac{dx_j\,(t)}{dt} = -\frac{x_j\,(t)}{\tau_{\text{NMDA,rise}}} + \sum_k \delta(t - t_j^k)$$

where the decay time of NMDA currents is taken to be $\tau_{NMDA,decay} = 100$ ms, $\alpha = 0.5$ ms^{-1}, and $\tau_{NMDA,rise} = 2$ ms (Hestrin et al., 1990; Spruston et al., 1995). Last, the GABA synaptic variable obeys

$$\frac{ds_j^{\text{GABA}}\,(t)}{dt} = -\frac{s_j^{\text{GABA}}\,(t)}{\tau_{\text{GABA}}} + \sum_k \delta(t - t_j^k)$$

where the decay time constant of GABA currents is taken to be $\tau_{GABA} = 5$ ms (Salin and Prince, 1996; Xiang et al., 1998). Note that

the very fast rise times (<1 ms) of both AMPA and GABA currents are neglected. All synapses have a latency of 0.5 ms.

I used the following values for the recurrent synaptic conductances (in nS) in the $N = 2000$ neurons network: for pyramidal cells, $g_{ext,AMPA} = 2.1$, $g_{rec,AMPA} = 0.05$, $g_{NMDA} = 0.165$, and $g_{GABA} = 1.3$; for interneurons, $g_{ext,AMPA} = 1.62$, $g_{rec,AMPA} = 0.04$, $g_{NMDA} = 0.13$, and $g_{GABA} = 1.0$. Note that these synaptic conductances correspond roughly to experimentally measured conductances (see for example, Destexhe et al., 1998, and references therein). Three features are noteworthy. First, recurrent excitation is assumed to be largely mediated by the NMDA receptors (Wang, 1999, 2001). Second, the network is overall dominated by recurrent inhibition (Amit and Brunel, 1997; Brunel and Wang, 2001). Third, neurons receive a large amount of stochastic background inputs. These three assumptions are important for the decision-making behavior of the model (see Results).

Structure of Recurrent Excitatory Connections between Pyramidal Cells

Each neuron receives inputs from all other neurons, but with structured synaptic weights. The coupling strength between a pair of neurons is prescribed according to a "Hebbian" rule: the synapse is strong (weak) if in the past the two cells tended to be active in a correlated (anticorrelated) manner. Hence, inside a selective population, $w_j = w_+$, where $w_+ > 1$ is a dimensionless parameter that is equal to the relative strength of "potentiated" synapses with respect to the baseline. Unless specified otherwise, I used $w_+ = 1.7$. Between two different selective populations, and from the nonselective population to selective ones, $w_j = w_-$, where $w_- < 1$ measures the strength of synaptic "depression." Other connections have $w_j = 1$. It is assumed that the spontaneous activity of neurons is largely unaffected by synaptic modifications, because synaptic depression compensates the effect of potentiation at the network level. More specifically, by choosing $w_- = 1 - f(w_+ - 1)/(1 - f)$, the overall recurrent excitatory synaptic drive in the spontaneous state remains constant as w_+ is varied (Amit and Brunel, 1997). Synaptic efficacies remain fixed through the simulation.

Population Firing Rate

The instantaneous population firing rates r_A and r_B were calculated as follows. For each time window of 50 ms, slided with a time step of 5 ms, the total spike number of each of the two neural groups is counted and divided by the neuron number and the time window.

Simulations

Computer simulations were run on a Linux workstation, using a modified RK2 routine (Hansel et al., 1998; Shelley and Tao, 2001) for the numerical integration of the coupled equations describing the dynamics of all cells and synapses, with integration time step $dt = 0.02$ ms.

For a given parameter set and each coherence level, the network's performance of decision-making behavior is assessed by estimating the percentage of correct choices averaged over n = 200–1000 trials.

Acknowledgments

I am indebted to Michael Shadlen and William Newsome for stimulating discussions and for sending me preprints. I also thank Michael Shadlen, Larry Abbott, Nicolas Brunel, and Paul Miller for comments on the manuscript. This work was supported by an NSF Career Award, NIMH, the A.P. Sloan Foundation, and the Swartz Foundation.

Received: July 16, 2002
Revised: October 7, 2002

References

Amit, D.J. (1995). The Hebbian paradigm reintegrated: local reverberations as internal representations. Behav. Brain Sci. *18*, 617–626.

Amit, D.J., and Brunel, N. (1997). Model of global spontaneous activity and local structured activity during delay periods in the cerebral cortex. Cereb. Cortex *7*, 237–252.

Bair, W., Zohary, E., and Newsome, W.T. (2001). Correlated firing in macaque visual area MT: time scales and relationship to behavior. J. Neurosci. *21*, 1676–1697.

Bisley, J.W., Zaksas, D., and Pasternak, T. (2001). Microstimulation of cortical area MT affects performance on a visual working memory task. J. Neurophysiol. *85*, 187–196.

Braitenberg, V., and Schütz, A. (1991). Anatomy of the Cortex. (Berlin: Springer-Verlag).

Britten, K.H., Shadlen, M.N., Newsome, W.T., and Movshon, J.A. (1992). The analysis of visual motion: a comparison of neuronal and psychophysical performance. J. Neurosci. *12*, 4745–4765.

Britten, K.H., Shadlen, M.N., Newsome, W.T., and Movshon, J.A. (1993). Responses of neurons in macaque MT to stochastic motion signals. Vis. Neurosci. *10*, 1157–1169.

Britten, K.H., Newsome, W.T., Shadlen, M.N., Celebrini, S., and Movshon, J.A. (1996). A relationship between behavioral choice and the visual responses of neurons in macaque MT. Vis. Neurosci. *13*, 87–100.

Brunel, N., and Wang, X.J. (2001). Effects of neuromodulation in a cortical network model of object working memory dominated by recurrent inhibition. J. Comput. Neurosci. *11*, 63–85.

Carpenter, R.H.S. (1981). Oculomotor procrastination. In Eye Movements: Cognition and Visual Perception (Hillsdale, NJ: Lawrence Erlbaum), pp. 237–246.

Carpenter, R.H.S., and Williams, M. (1995). Neural computation of log likelihood in control of saccadic eye movements. Nature *377*, 59–62.

Chafee, M.V., and Goldman-Rakic, P.S. (1998). Neuronal activity in macaque prefrontal area 8a and posterior parietal area 7ip related to memory guided saccades. J. Neurophysiol. *79*, 2919–2940.

Colby, C.L., Duhamel, J.R., and Goldberg, M.E. (1996). Visual, presaccadic, and cognitive activation of single neurons in monkey lateral intraparietal area. J. Neurophysiol. *76*, 2841–2852.

Compte, A., Brunel, N., Goldman-Rakic, P.S., and Wang, X.-J. (2000). Synaptic mechanisms and network dynamics underlying spatial working memory in a cortical network model. Cereb. Cortex *10*, 910–923.

Cook, E.P., and Maunsell, J.H.R. (2002). Dynamics of neuronal responses in macaque MT and VIP during motion detection. Nat. Neurosci. *5*, 985–994.

Destexhe, A., Mainen, Z.F., and Sejnowski, T.J. (1998). Kinetic models of synaptic transmission. In Methods in Neuronal Modeling, Second Edition, C. Koch and I. Segev, eds. (Cambridge, MA: MIT Press), pp. 1–25.

Ditterich, J., Mazurek, M.E., Roitman, J.D., Palmer, J., and Shadlen, M.N. (2001). A computational model of the speed and accuracy of motion discrimination. In *Society for Neuroscience Abstracts*, Volume 27, 58.12.

Dodd, J.V., Krug, K., Cumming, B.G., and Parker, A.J. (2001). Perceptually bistable 3-d figures evoke high choice probabilities in cortical area MT. J. Neurosci. *21*, 4809–4821.

Gnadt, J.W., and Andersen, R.A. (1988). Memory related motor planning activity in posterior parietal cortex of macaque. Exp. Brain Res. *70*, 216–220.

Gold, J.I., and Shadlen, M.N. (2001). Neural computations that underlie decisions about sensory stimuli. Trends Cogn. Sci. *5*, 10–16.

Hansel, D., Mato, G., Meunier, C., and Neltner, L. (1998). On numerical simulations of integrate-and-fire neural networks. Neural Comput. *10*, 467–483.

Hastie, R. (2001). Problems for judgment and decision making. Annu. Rev. Psychol. *52*, 653–683.

Hernández, A., Zainos, A., and Romo, R. (2002). Temporal evolution of a decision making process in medial premotor cortex. Neuron *33*, 950–972.

Hertz, J., Krogh, A., and Palmer, R.G. (1991). Introduction to the Theory of Neural Computation (Reading, MA: Addision-Wesley Publishing Company).

Hestrin, S., Sah, P., and Nicoll, R. (1990). Mechanisms generating

the time course of dual component excitatory synaptic currents recorded in hippocampal slices. Neuron *5*, 247–253.

Jahr, C.E., and Stevens, C.F. (1990). Voltage dependence of NMDA-activated macroscopic conductances predicted by single-channel kinetics. J. Neurosci. *10*, 3178–3182.

Kim, J.-N., and Shadlen, M.N. (1999). Neural correlates of a decision in the dorsolateral prefrontal cortex of the macaque. Nat. Neurosci. *2*, 176–183.

Krauzlis, R., and Dill, N. (2002). Neural correlates of target choice for pursuit and saccades in the primate superior colliculus. Neuron *35*, 355–363.

Luce, R.D. (1986). Response Time: Their Role in Inferring Elementary Mental Organization (New York: Oxford University Press).

McCormick, D., Connors, B., Lighthall, J., and Prince, D. (1985). Comparative electrophysiology of pyramidal and sparsely spiny stellate neurons in the neocortex. J. Neurophysiol. *54*, 782–806.

Newsome, W.T., Britten, K.H., and Movshon, J.A. (1989). Neuronal correlates of a perceptual decision. Nature *341*, 52–54.

Parker, A.J., and Newsome, W.T. (1998). Sense and the single neuron: probing the physiology of perception. Annu. Rev. Neurosci. *21*, 227–277.

Platt, M.L. (2002). Neural correlates of decisions. Curr. Opin. Neurobiol. *12*, 144–148.

Platt, M.L., and Glimcher, P.W. (1999). Neural correlates of decision variables in parietal cortex. Nature *400*, 233–238.

Quintana, J., and Fuster, J.M. (1992). Mnemonic and predictive functions of cortical neurons in a memory task. Neuroreport *3*, 721–724.

Quintana, J., and Fuster, J.M. (1999). From perception to action: temporal integrative functions of prefrontal and parietal neurons. Cereb. Cortex *9*, 213–221.

Ratcliff, R. (1978). A theory of memory retrieval. Psychol. Rev. *85*, 59–108.

Ratcliff, R., Zandt, T.V., and McKoon, G. (1999). Connectionist and diffusion models of reaction time. Psychol. Rev. *106*, 261–300.

Reddi, B., and Carpenter, R.H. (2000). The influence of urgency on decision time. Nat. Neurosci. *3*, 827–831.

Roitman, J.D., and Shadlen, M.N. (2002). Response of neurons in the lateral intraparietal area (LIP) during a combined visual discrimination reaction time task. J. Neurosci. *22*, 9475—9489.

Romo, R., and Salinas, E. (2000). Touch and go: decision-making mechanisms in somatosensation. Annu. Rev. Neurosci. *24*, 107–137.

Romo, R., Zainos, A., and Hernández, A. (1997). Categorical perception of somesthetic stimuli: psychophysical measurements correlated with neuronal events in primate medial premotor cortex. Cereb. Cortex *7*, 317–326.

Salin, P.A., and Prince, D.A. (1996). Spontaneous $GABA_A$ receptor mediated inhibitory currents in adult rat somatosensory cortex. J. Neurophysiol. *75*, 1573–1588.

Salzman, C.D., Britten, K.H., and Newsome, W.T. (1990). Cortical microstimulation influences perceptual judgments of motion direction. Nature *346*, 174–177.

Schall, J.D. (2001). Neural basis of deciding, choosing and acting. Nat. Neurosci. *2*, 33–42.

Schall, J.D., Hanes, D.P., Thompson, K.G., and King, D.J. (1995). Saccade target selection in frontal eye field of macaque. I. Visual and premovement activation. J. Neurosci. *15*, 6905–6918.

Scherzer, C.R., Landwehrmeyer, G.B., Kerner, J.A., Counihan, T.J., Kosinski, C.M., Standaert, D.G., Daggett, L.P., Velicelebi, G., Penney, J.B., and Young, A.B. (1998). Expression of N-methyl-D-aspartate receptor subunit mRNAs in the human brain: hippocampus and cortex. J. Comp. Neurol. *390*, 75–90.

Seung, H.S. (1996). How the brain keeps the eyes still. Proc. Natl. Acad. Sci. USA *93*, 13339–13344.

Seung, H.S., Lee, D.D., Reis, B.Y., and Tank, D.W. (2000). Stability of the memory of eye position in a recurrent network of conductance-based model neurons. Neuron *26*, 259–271.

Shadlen, M.N., and Newsome, W.T. (1996). Motion perception: seeing and deciding. Proc. Natl. Acad. Sci. USA *93*, 628–633.

Shadlen, M.N., and Newsome, W.T. (2001). Neural basis of a perceptual decision in the parietal cortex (area LIP) of the rhesus monkey. J. Neurophysiol. *86*, 1916–1936.

Shadlen, M.N., Britten, K.H., Newsome, W.T., and Movshon, J.A. (1996). A computational analysis of the relationship between neuronal and behavioral responses to visual motion. J. Neurosci. *15*, 3870–3896.

Shelley, M., and Tao, L. (2001). Efficient and accurate time-stepping schemes for integrate-and-fire neuronal networks. J. Comput. Neurosci. *11*, 111–119.

Simoncelli, E.P., and Heeger, D.J. (1998). A model of neuronal responses in visual area MT. Vision Res. *38*, 743–761.

Spruston, N., Jonas, P., and Sakmann, B. (1995). Dendritic glutamate receptor channel in rat hippocampal CA3 and CA1 pyramidal neurons. J. Physiol. *482*, 325–352.

Tsodyks, M.V., and Sejnowski, T. (1995). Rapid state switching in balanced cortical network models. Network *6*, 111–124.

Tuckwell, H.C. (1988). Introduction to Theoretical Neurobiology (Cambridge: Cambridge University Press).

Turrigiano, G. (1999). Homeostatic plasticity in neuronal networks: the more things change, the more they stay the same. Trends Neurosci. *22*, 221–227.

Usher, M., and McClelland, J. (2001). On the time course of perceptual choice: the leaky competing accumulator model. Psychol. Rev. *108*, 550–592.

van Vreeswijk, C., and Sompolinsky, H. (1998). Chaotic balanced state in a model of cortical circuits. Neural Comput. *10*, 1321–1371.

Wang, X.-J. (1999). Synaptic basis of cortical persistent activity: the importance of NMDA receptors to working memory. J. Neurosci. *19*, 9587–9603.

Wang, X.-J. (2001). Synaptic reverberation underlying mnemonic persistent activity. Trends Neurosci. *24*, 455–463.

Xiang, Z., Huguenard, J.R., and Prince, D.A. (1998). $GABA_A$ receptor mediated currents in interneurons and pyramidal cells of rat visual cortex. J. Physiol. *506*, 715–730.

Zohary, E., Shadlen, M.N., and Newsome, W.T. (1994). Correlated neuronal discharge rate and its implications for psychophysical performance. Nature *370*, 140–143.